Can. J. Remote Sensing, Vol. 28, No. 2, pp. 275–290, 2002

Detecting spatial and temporal patterns in NDVI time series using histograms

María Margarita González Loyarte

Abstract. The aim of this study was to analyse bimodal histogram patterns of monthly National Oceanic and Atmospheric Administration (NOAA) advanced very high resolution radiometer (AVHRR) normalized difference vegetation index (NDVI) global area coverage (GAC) data and their relation to vegetation dynamics and climatic conditions for the period 1982–1991 in Argentina. The proposed method was to split up bimodal histograms by the median criterion and to study each mode as a separate unimodal frequency distribution. Modes were analysed based on their histogram shape and statistical parameters, geographical distribution and dynamics, and climatic significance. For the latter, a multinomial statistical analysis was used. The split-up criterion yielded coherent results. Histogram shapes and statistical parameters changed according to season. For geographical dynamics, 84% of pixels remained in the same mode through the seasons, and 16% shifted temporarily to the other mode. Changes from low-NDVI mode to high-NDVI mode were caused by an improvement in water supply, rainfall or irrigation, and higher temperatures. Changes in the opposite direction were due to a reduction in vegetation cover produced by drought, harvest, or autumn effects. The low-NDVI mode was strongly related to the arid zone with 74.6% probability ($\alpha = 0.05$), and the high-NDVI mode was related to humid (58.8%) and semiarid zones (38.4%). This contribution helps explain the dynamics of vegetation cover along the latitudinal range from 22° to 55°S, for nine growing cycles, with a simple methodology. Improving the knowledge of multimodal histograms may allow a better understanding of difficult classification results.

Résumé. Le but a été d'analyser les patrons des histogrammes bimodaux correspondantes aux données mensuelles NOAA AVHRR NDVI GAC et leur rapport avec la dynamique de la végétation et les conditions climatiques, pour la période 1982–1991 en Argentine. La méthode proposée a été couper les histogrammes bimodaux par la médiane pour étudier chaque mode séparement comme une distribution unimodale des fréquences. Les modes ont été étudiées par la forme des histogrammes et par leur statistiques, par leur distribution géographique et leur dynamique, et par leur rapport avec les conditions climatiques. Ce dernier a été étudié par une analyse statistique multinomiale. Le critère de coupe par la médiane a donné des résultats cohérents. Les formes des histogrammes ainsi que les statistiques ont été modifiées selon les saisons. En ce qui concerne la dynamique géographique, 84% des pixels sont restés dans la même mode à travers les saisons, le reste a changé temporairement à l'autre mode. Les changements de la mode des bas NDVI à celle des haut NDVI ont été expliqué par l'amélioration dans l'approvisonement de l'eau, soi par les pluies ou par l'irrigation, et par des températures plus elevées. Les changements contraires ont été dus à la reduction du couvert végétale à cause de sécheresses, récoltes ou l'arrivé de l'automne. La mode aux bas NDVI a été fortement associée au zone aride avec 74,6% de probabilité ($\alpha = 0{,}05$) tandis que la mode avec haut NDVI a été associée aux zones humides (58,8%) et semiarides (38,4%). Cette contribution a aidé à comprendre la dynamique du couvert végétal au long de 33 degrées de latitude pour neuf cycles végétatives avec une méthode simple. L'amélioration de la connaissance sur les histogrammes bimodaux peut aider à mieux comprendre les résultats des classifications difficiles.

Introduction

The histogram is a useful and straightforward graphic representation of the information content of an image and provides the user with an appreciation of the quality of the original data (e.g., whether it is low or high in contrast or multimodal in nature) (Jensen, 1989). A multimodal histogram presents two or more modes, each with a peak (highest frequency) and a valley between modes (lowest frequency). Various peaks and valleys in a multimodal histogram may correspond to dominant types of land cover in an image (Jensen, 1989). This study focused on understanding the ecological significance of modes at the regional scale.

There are many research works showing the usefulness of National Oceanic and Atmospheric Administration (NOAA) advanced very high resolution radiometer (AVHRR) normalized difference vegetation index (NDVI) data in studies at a regional scale. These works cover aspects like the relationship between phenology and rainfall (Justice et al., 1985, 1991; Azzali, 1990; Tucker et al., 1991; González Loyarte and Menenti, 2000) or biomass evaluation and modelling (Diallo et al., 1991; Wylie et al., 1991; Franklin and Hiernaux, 1991). NDVI monthly data are also useful to express vegetation dynamics through Fast Fourier analysis (Menenti et al., 1991; Azzali and Menenti, 1999, 2000; González Loyarte, 1996). None of these authors commented on the histogram patterns of NDVI data. Would multimodal histograms of NDVI

Received 18 December 2000. Accepted 18 January 2002.

M.M. González Loyarte. Argentinian Institute for Research on Arid Zones (IADIZA/CRICYT), National Council for Scientific and Technical Research (CONICET), P.O. Box 507, 5500 Mendoza, Argentina (e-mail: gloyarte@lab.cricyt.edu.ar).

data be a phenological indicator of vegetation response to climatic conditions at the regional scale?

Argentinian arid and semiarid areas cover 75% of the country. Different authors (De Martonne, 1948; Bruniard, 1982) considered the arid regions as the consequence of degradation and impoverishment of humid zones. Bruniard (1982) studied the "Argentinian arid diagonal" and concluded that the humid climates (northern and southern) would degrade progressively toward maximal aridity. This axis of maximal aridity divides the rainfall areas associated with the Atlantic (rains in spring–summer) and Pacific (rains in autumn–winter) anticyclones, respectively (**Figure 1**). The subset of monthly NOAA AVHRR NDVI global area coverage (GAC) images used to study vegetation cover in Argentina (González Loyarte, 1996) showed bimodal histograms throughout the time series of available observations. Are these two modes associated with these rainfall areas?

This study aims at answering this question and others such as the following: Is it possible to describe vegetation cover dynamics by histogram analysis? Are the observed histogram modes associated with north–south climatic conditions? Are these modes constant along an NDVI time series? Is there a constant criterion to separate the modes? Is there a constant geographical distribution of pixels of each mode within growing cycles?

This paper deals with the analysis of histogram patterns of 9-year monthly NOAA AVHRR NDVI GAC data and their relationship to vegetation dynamics and climatic conditions in Argentina. Three main aspects were analysed: histogram patterns, geographical distribution and dynamics of both modes, and the climatic significance of both modes. In relation to histogram patterns, changes in the shape of monthly histograms for two growing cycles were analysed. Also, each monthly bimodal histogram was split into two modes by the median, and the statistics of each mode (mean and standard deviation) were analysed. For geographical distribution, the spatial distribution of each mode and the spatial changes of modes from one season to another were analysed. For this analysis, four monthly images per growing cycle were selected as being representative of each season. Lastly, the climatic significance of each mode was studied using a multinomial statistical analysis. The main results were that the shape of histograms across growing cycles followed the changes in brightness as a response to environmental conditions like droughts. The spatial distribution of the modes across growing cycles and the temporary shift (dynamics) from one mode to the other were in agreement with seasonal changes, water availability, and crop management. Both modes responded to climatic conditions, arid and semiarid–humid, regardless of the north–south rainfall areas.

Materials

The study was based on monthly NOAA AVHRR NDVI composite images collected for South America over a 10 year period. These were GAC data with a spatial resolution of 7.6 km produced by the National Aeronautics and Space Administration (NASA) and obtained in the framework of the Netherlands Remote Sensing Board project *Fourier analysis of temporal NDVI in the Southern African and American continents* (Azzali and Menenti, 1996). A subset of 108 monthly NDVI images from July 1982 to June 1991 were used. These images covered nine growing cycles.

A climatic map was digitized and registered to NDVI images (**Figure 1**). This map was in agreement with the agro-economic criterion on agricultural activity reported by Roig et al. (1988, 1992). Definitions of each climatic condition were rain-fed agriculture (humid), marginal and hazardous rain-fed agriculture where dry farming was needed (semiarid), and areas where agriculture was possible only with irrigation (arid). These areas were drawn based on mean annual rainfall and temperature limits. Isohyets and isotherms were extracted from the climatic atlas of Hoffmann (1975). Five climatic zones were distinguished for this analysis: (1) arid (<250–300 mm rainfall per year and mean annual temperatures from <10°C to 20°C, including both rainfall areas), (2) northern semiarid (300 to 700–800 rainfall per year and mean annual temperatures from 15°C to >20°C), (3) southern semiarid (250–600 mm rainfall per year and mean annual temperatures below 10°C), (4) northern humid (>700–800 mm rainfall per year and mean annual temperatures from 15°C to >20°C), and (5) southern

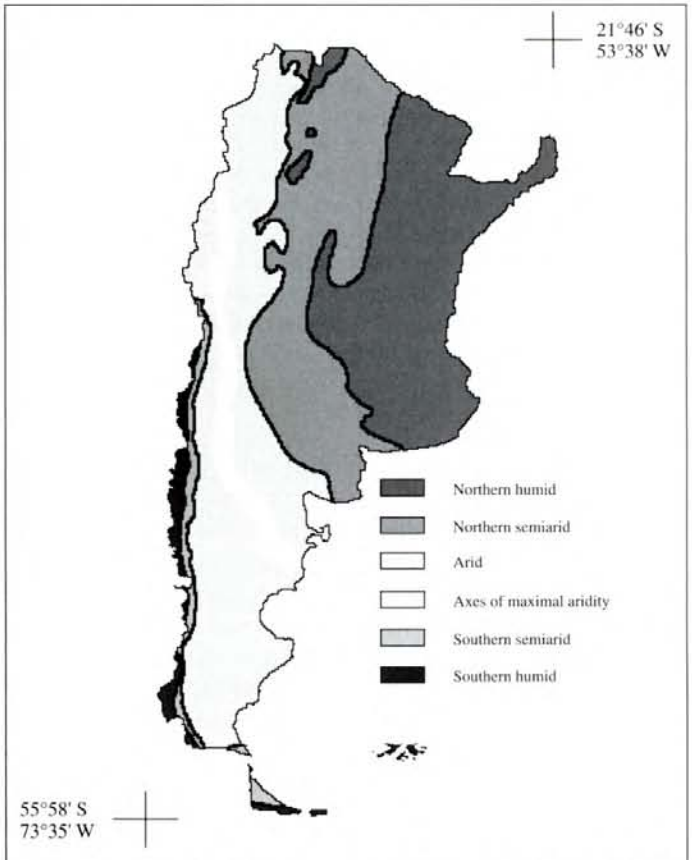

Figure 1. Map of the climatic zones of Argentina. Adapted from Bruniard (1982) and González Loyarte (1995).

humid (>600 mm rainfall per year and mean annual temperatures below 10°C).

Specific software packages included ERDAS 7.5 (PC) for image processing, STATISTICA for standard statistical analysis, and MULTINOM for multinomial analysis (Diblasi, 1999; made under the MATLAB framework).

Methods

Data preparation

The subset of 108 monthly NDVI images were masked for the Argentinian territory and their frequency distributions (histograms) were analysed.

For the frequency distribution analysis, NDVI ASCII data (digital number DN) from each image were obtained. Once data were imported in STATISTICA, value 0 (background) and value 255 (noise) were excluded (cleaned) by subsetting. The noise came from ancillary data (political boundaries, rivers, coordinates) that were incorporated as NDVI values (artefacts) when transforming images from 16 to 8 bits. Statistics for cleaned data were calculated (mean, median, mode, variance, standard deviation).

The climatic map with five climatic zones was digitized and registered to the NDVI images.

Histogram pattern analysis: dynamics and separation of the two modes

Dynamics of monthly bimodal histograms for selected growing cycles

Monthly bimodal histograms for selected cycles were plotted along with reference lines for detecting dynamics. This reflected the changes in shape in the monthly histograms through the growing cycle. From the set of 108 NDVI cleaned data files, those corresponding to two growing cycles were selected: 1982–1983, regarded as the normal cycle, and 1987–1988, regarded as an example of an irregular cycle with droughts in northern Argentina (González Loyarte and Menenti, 2000).

Although this set had already been cloud screened, a more refined procedure identified a number of cloud–snow contaminated pixels, which were excluded from the analysis.

Splitting up bimodal histograms into subsets A and B

The two portions corresponding to the two peaks (modes) observed in the histogram were extracted from each bimodal histogram of monthly NDVI data. Each mode was studied as a new unimodal distribution.

Analysing frequency distributions, it was concluded that the median values were a suitable criterion to divide the two modes of the histograms because medians were always in the valley between both peaks. Therefore, cleaned data were split up into two subsets by the corresponding median. Subset A included from the minimum digital numbers to the median, and subset B included all digital numbers larger than the median (**Figure 2**). The median was always assigned to subset A. Peaks A and B will be referred to hereafter as subsets or modes. For subsets A and B, statistics were calculated (mean, median, mode, standard deviation, variance). This operation was repeated for the 108 cleaned NDVI ASCII data files. Monthly means and standard deviations for bimodal histograms and for subsets A and B were plotted.

Geographical distribution of the two modes of bimodal histograms and its dynamics across selected growing cycles

Geographical distribution of subsets A and B

The process to obtain the geographical distribution of subsets A and B was to recode the digital numbers (DN) of the NDVI images. Before recoding, each image (.LAN) was copied as a geographical information system (GIS) file (.GIS) with 256 classes. Recoding of images was carried out according to their median (Md) as follows (**Figure 2**): (1) subset A = DN ≤ Md (excluding 0) was assigned the new value 1, (2) subset B = DN > Md was assigned the new value 2, and (3) ancillary data with DN = 255 were excluded by recoding as 0. Thus, subsets A and B in histograms correspond to classes A and B in maps.

To understand the geographical distribution and dynamics of subsets A and B through the growing cycle, a monthly image was selected as being representative of each season (Southern Hemisphere): July for winter, October for spring, January for summer, and April for autumn. Each representative seasonal NDVI image was recoded to obtain the classes A and B. Maps of classes A and B for each season and for the selected cycles (1982–1983 and 1987–1988) were generated.

Dynamics of A–B geographical distribution

For the two selected cycles (1982–1983 and 1987–1988) each A–B seasonal image was crossed with the image of the preceding season (ERDAS/MATRIX). Thus, three comparisons per cycle were made: winter–spring, spring–summer, and summer–autumn. Results reflecting whether pixels A and B remained in the same class, A or B, or changed class from one season to the next were presented in maps and in tabular form.

Classes A and B changes between seasons were evaluated with the support of a previous land use map based on the classification of vegetation dynamics by Fourier parameters (González Loyarte, 1996). From this map some classes were selected to explain changes. The selected classes were related to agriculture under irrigation (oases), rain-fed agriculture, or a combination of agriculture and grasslands for grazing. Also, arid and semiarid woodlands and southern mountain forests, shrubby steppe, and grassy steppe were considered.

Climatic significance of bimodal histograms: multinomial statistical analysis of subsets A and B

The relationship between climatic conditions and the A–B geographical patterns was examined. The objective of the analysis was to find out whether a given pixel remained in the same climatic zone, independently of the season.

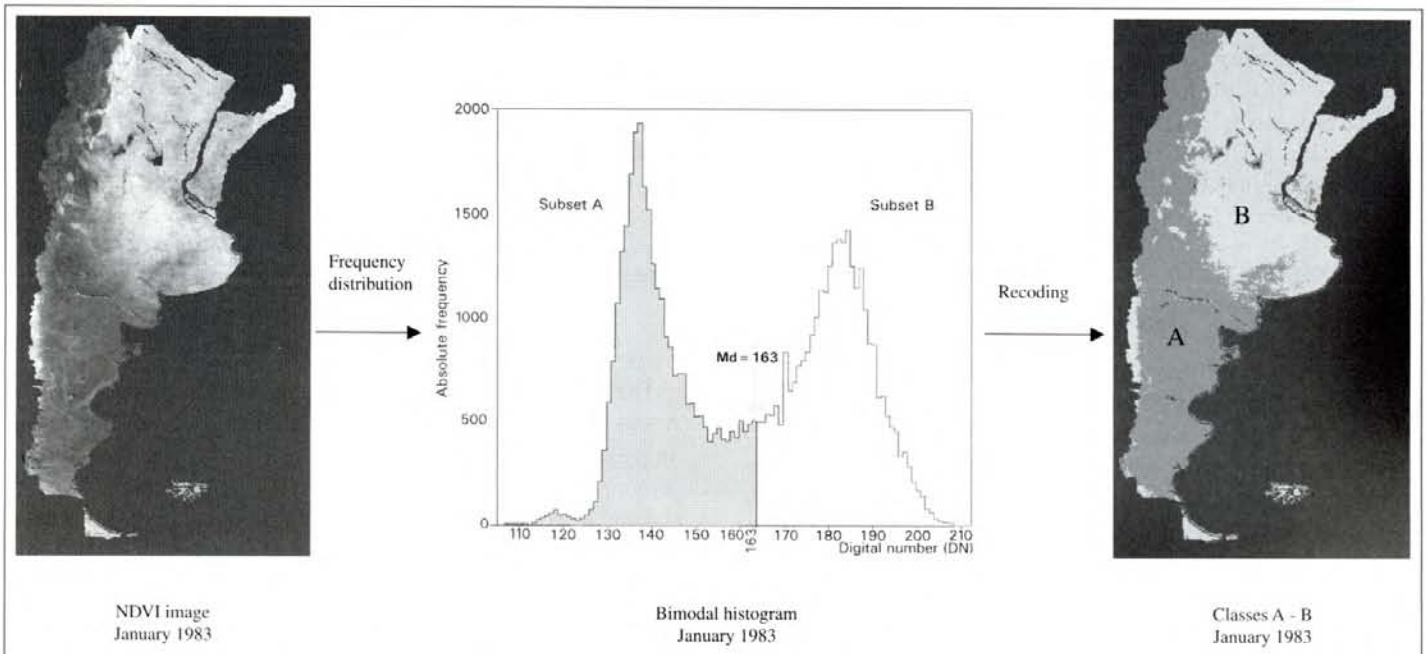

Figure 2. Example of the process of splitting up bimodal histograms and transforming NDVI images into A–B images by recoding. Md, median.

Climatic zones were analysed together with each A–B season map. Crossed analyses of the corresponding images were made with ERDAS/SUMMARY. These analyses were made for all four seasons and for the nine growing cycles (36 A–B maps). Results, indicating frequencies of pixels A and B in each climatic zone for each season, were analysed by a simultaneous statistical procedure (multinomial analysis) to estimate the probability that pixels A and B belong to a climatic zone.

The multinomial analysis was a simultaneous statistical comparison of the frequency of classes A and B, separately, for the seasons and climatic zones along each growing cycle. Thus, there were two classification criteria, namely time (r = 4 seasons, regarded as populations) and climatic conditions (c = 5 climatic zones, regarded as categories). When taken together, all observations formed an $r \times c$ (4 × 5) contingency table. The probability for each is (Miller, 1981) P_{ij} for i = 1, ..., 4 (seasons) and j = 1, ..., 5 (climatic zones), that is, P_{ij} is the probability of the ith population (season) in the jth category (climatic zone), where the null hypothesis H_0 is tested against the alternative hypothesis H_1 as follows:

$$H_0: P_{ij} = P_{kj}; \quad j = 1, \ldots, 5; \; i, k = 1, \ldots, 4 \; (i \neq k)$$

and

$$H_1: P_{ij} \neq P_{kj}$$

for at least one pair (i, k) of populations in a jth category.

The null hypothesis H_0 was that the probability structure over categories did not change from season to season, within a growing cycle, which meant that each pixel would keep its probability of belonging to a certain climatic category through seasons. Thus, seasonal changes in rain-fed values would not modify the probability of belonging to a certain climatic zone, for each subset, A or B. The alternative hypothesis H_1 indicated that there was at least a pair of seasons where the probabilities to belong to a certain climatic zone were different within a growing cycle.

Estimated probabilities, calculated by the MULTINOM program (Diblasi, 1999), were as follows:

$$\hat{P}_{ij} = \frac{n_{ij}}{n_{i\bullet}}; \qquad j = 1, 2, 3, 4, 5 \text{ and } i = 1, 2, 3, 4$$

where n_{ij} is the number of pixels for season i and zone j, and $n_{i\bullet}$ is the total number of pixels within the ith season

Results

Histogram pattern analysis: dynamics and separation of the two modes

Dynamics of monthly bimodal histograms for selected growing cycles

Monthly bimodal histograms of the selected growing cycles (1982–1983 and 1987–1988) are presented in **Figure 3**. Common straight lines corresponding to peaks A and B of July 1982 were drawn to help in comparing the changes

Bimodal histograms showed similarities and differences along both cycles. The median increased during the cycle, reaching its maximum in summer and its minimum in winter.

Considering the straight lines from peaks A and B from July 1982 to June 1983, the peak of subset A (line on the left) clearly kept an almost constant position (DN) during the whole growing cycle. The peak of subset B (line on the right) clearly

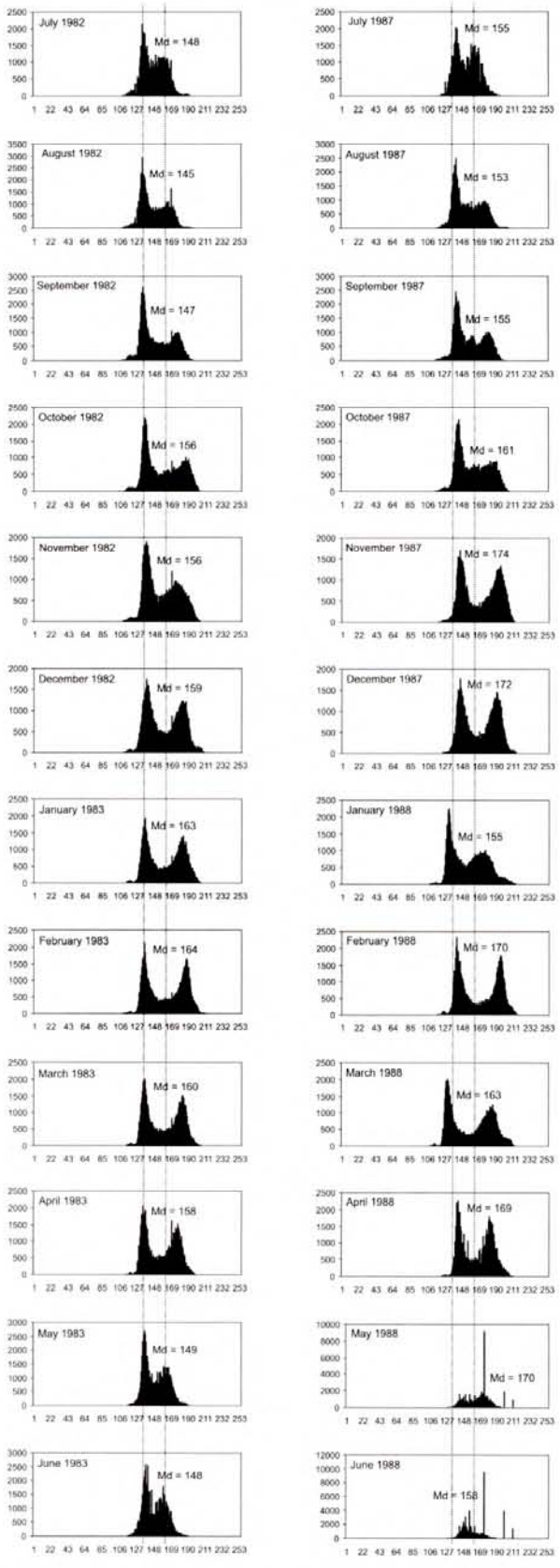

Figure 3. Comparative evolution of monthly bimodal histograms for selected growth cycles, 1982–1983 and 1987–1988. The *x* axis gives the NDVI digital number (DN), and the *y* axis gives the absolute frequency (number of pixels for each DN).

grew and shifted to a higher DN, accentuating the bimodal nature of histograms during summer and early fall (December 1982 to April 1983).

During the 1987–1988 cycle there were some differences in behaviour. The peak of mode A remained constant except for January and March 1988, during which it shifted toward lower values of NDVI as did peak B. Histograms corresponding to May and June 1988 showed a significant distortion of NDVI values in southern Argentina. These are artefacts with unusually bright values.

Splitting up bimodal histograms into subsets A and B: monthly evolution of statistics

After splitting up bimodal histograms into subsets A and B, each subset was regarded as a new unimodal distribution. Statistics of each subset were calculated. Nine year monthly means and standard deviation, for bimodal histograms and for subsets A and B, were plotted (**Figure 4**).

By definition of subsets A and B, subset A showed lower mean values of NDVI than subset B, and both followed the rhythm of growing cycles. As expected, variations in standard deviation were much higher for bimodal histograms than for unimodal distributions of the separate subsets A and B.

Geographical distribution of the two modes of bimodal histograms and their dynamics across selected growing cycles

Geographical distribution of subsets A and B

The geographical distribution of subsets A and B was mapped at the country level, despite the small size of maps, to show the large-scale patterns of subsets A and B. The transformation of selected NDVI images was made by recoding them in classes A or B according to their medians (**Figure 2**). Four selected months (July, October, January, and April), representative of seasons, were mapped for the selected growing cycles (1982–1983 and 1987–1988) (**Figure 5**). Limits of climatic zones were added to the maps (**Figure 1**).

From a visual analysis, it was clear that class A was spatially related to the arid zone and part of semiarid areas. In contrast, class B was related to humid and semiarid zones.

During winter in southern Argentina (Patagonia), NDVI values were zero because of snow cover; and they were assigned the same white colour as the background. From spring to autumn, some patches of class B appeared in the middle of class A, coinciding with the important oases in the arid zone of central western Argentina. Despite the small scale of the maps, differences in A–B distribution from one season to another were detected.

Dynamics of A–B geographical distribution

The spatial changes in classes A and B from one season to the other were mapped (**Figure 6**). Each season, beginning with spring, was compared with the preceding season to detect whether pixels in classes A or B remained in the same class or shifted to the other class. Thus, changes were detected from

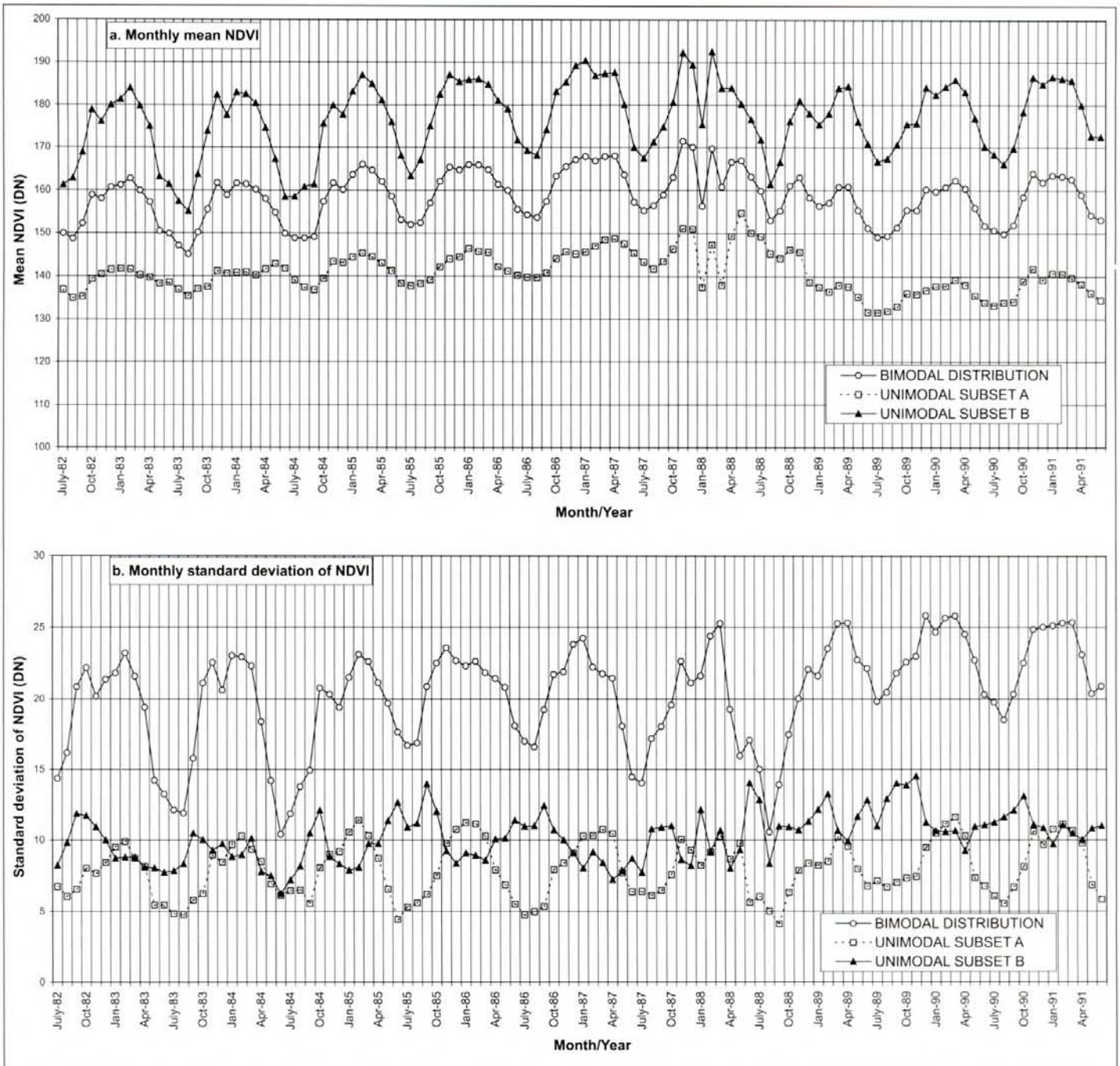

Figure 4. Evolution of monthly mean (a) and standard deviation (b) of the NDVI values for the bimodal distribution and unimodal subsets A and B.

winter to spring, from spring to summer, and from summer to autumn. Some areas showed similar changes in both growing cycles and others did not. The percentage of pixels that presented geographical coincidence or disagreement in classes was calculated (**Table 1**).

Climatic significance of bimodal histograms: multinomial statistical analysis of subsets A and B

The climatic significance of subsets A and B was analysed with the multinomial analysis. This analysis was repeated for each growing cycle. The null hypothesis stated that the probability of pixels in subsets A or B belonging to a certain climatic zone did not change from season to season within a growing cycle. The null hypothesis was rejected ($\alpha = 0.05$) for most of the cycles. This meant that the probability of subsets A or B belonging to a certain climatic zone was significantly different for two or more seasons. Thus, a seasonal influence on the distribution of A and B was expected.

The null hypothesis was accepted only for two growing cycles for subset A and for three cycles for subset B. For subset A, probabilities were not significantly different within the 1983–1984 and 1986–1987 cycles for the arid zone. For subset B, probabilities were not significantly different within the

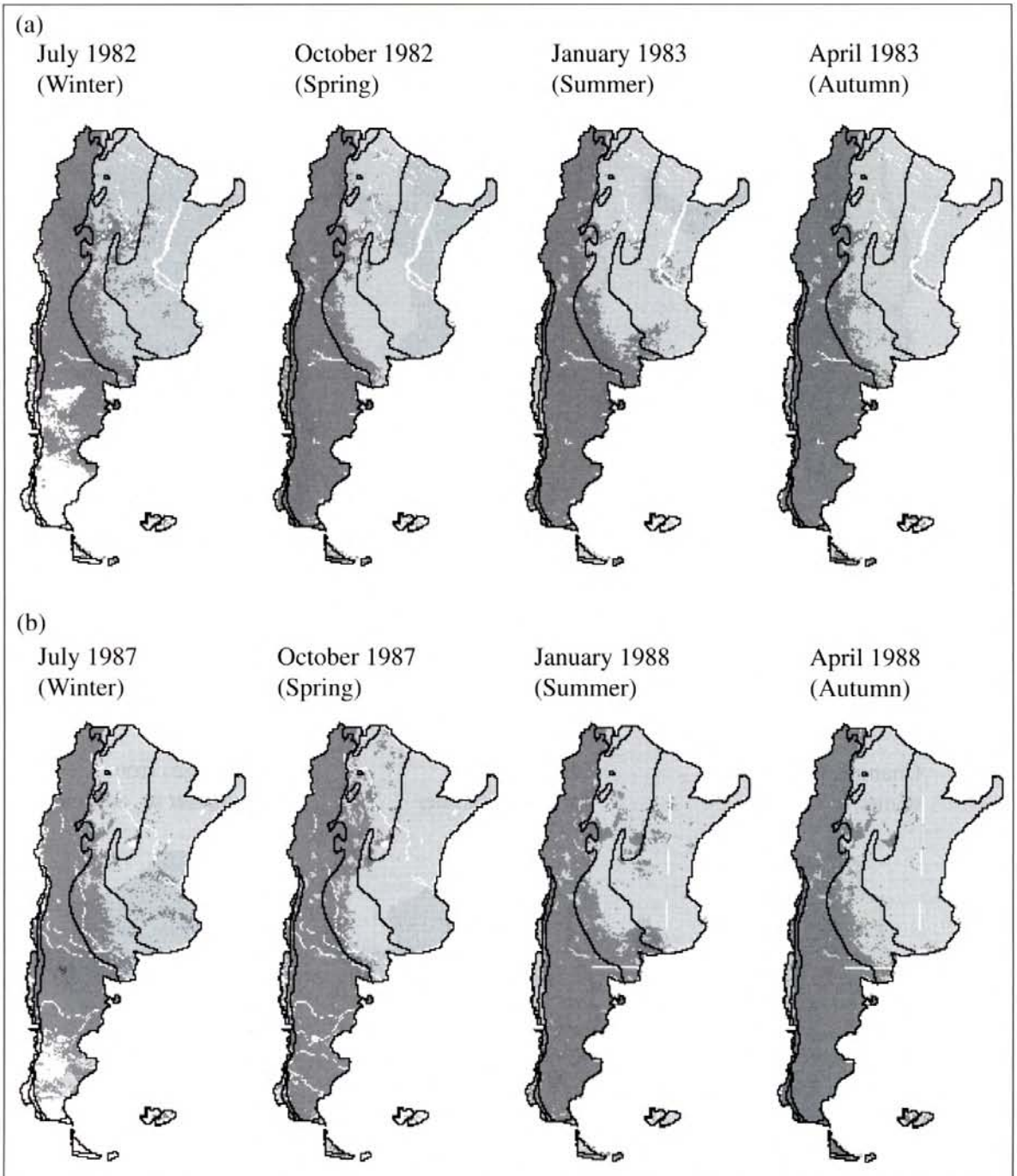

Figure 5. Geographical distribution of classes A (dark gray) and B (light gray) for the different seasons of the 1982–1983 (a) and 1987–1988 (b) growing cycles. Black lines are the limits of climatic zones.

1986–1987, 1989–1990, and 1990–1991 cycles for the northern humid zone. Estimated probabilities of pixels in subset A or subset B belonging to climatic zones for each season are plotted in **Figure 7**.

As an example, the estimated probability of subset A belonging to the arid zone was 0.6977 in the winter, 0.7849 in the spring, 0.7611 in the summer, and 0.7890 in the autumn of the 1982–1983 cycle (**Figure 7a**). This situation was similar for seasons of all cycles except for the winters of 1984 and 1988 where, due to cloud artefacts, the probability in Patagonia dropped to 0.4633. The impact of these artefacts was illustrated by the histograms for May and June 1988 (**Figure 3**).

Considering subset B for the 1982–1983 cycle, it is clear that pixels had a higher probability of belonging to the northern humid zone: 0.6127 in winter to 0.5393 in summer (**Figure 7b**). This probability changes significantly according to season. For the whole 1982–1983 cycle, pixels of subset B presented an average probability of 58.13% of belonging to humid zones

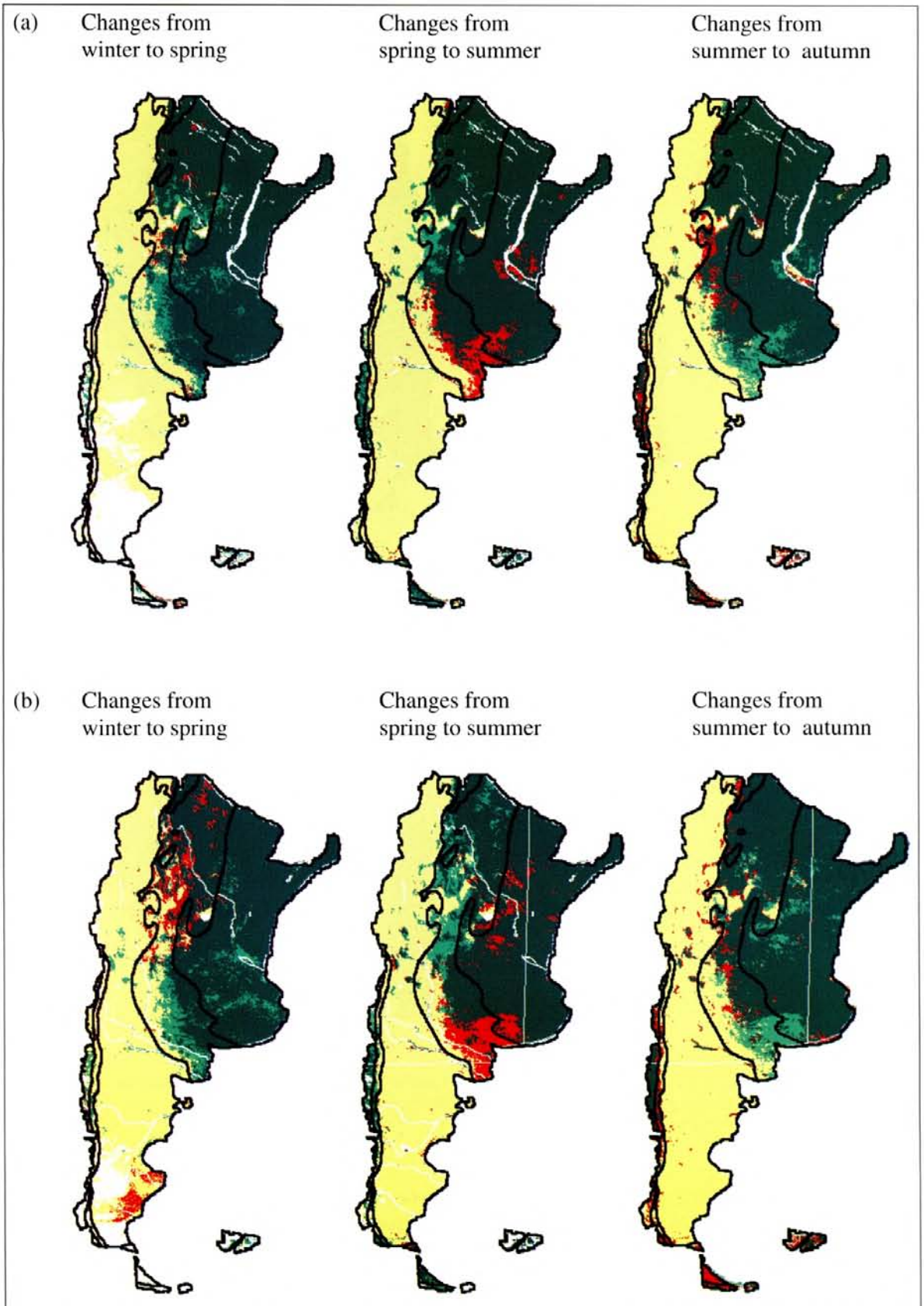

Figure 6. Geographical changes from one season to the next for the 1982–1983 (a) and 1987–1988 (b) growing cycles. The colours denote the following: changed from class A to class B (light green), changed from class B to class A (red), maintained as class A (yellow), and maintained as class B (dark green).

Table 1. Percentage of pixels in classes A and B that remained in the same class and pixels that changed from one class to another, from one season to the next for selected growing cycles, 1982–1983 and 1987–1988.

		October 1982 (Spring)			January 1983 (Summer)			April 1983 (Autumn)	
Classes	Month	A	B	Month	A	B	Month	A	B
A	July 1982	42.5	7.4	October 1982	45.3	4.7	January 1983	45.8	4.5
B	(Winter)	1.4	48.7	(Spring)	4.9	45.1	(Summer)	4.1	45.7
		October 1987 (Spring)			January 1988 (Summer)			April 1988 (Autumn)	
		A	B		A	B		A	B
A	July 1987	43.2	7.2	October 1987	43.5	7.9	January 1988	44.4	5.8
B	(Winter)	5.6	44.0	(Spring)	6.5	42.1	(Summer)	5.8	43.9

(northern and southern) and 40.16% of belonging to semiarid zones. This made a total of 98.29% of estimated probabilities of pixels of subset B belonging to semiarid–humid areas.

The average probability over the 9 years of subsets A and B belonging to each climatic zone was calculated (**Table 2**). These results were similar to those found for the 1982–1983 cycle.

Error evaluation

The source of detected errors was artefacts in the original data. These artefacts had an influence on the split-up criterion used. Artefacts originated from snow and cloud cover, ancillary data, and no valid land observations where higher NDVI values than usual were present. An attempt was made to reduce this error by eliminating the first two artefacts from the numerical analysis and from image analysis by image recoding. Therefore, images presented a different number of pixels each month. This error was estimated by considering the number of pixels with valid NDVI values for each image, including artefacts with higher NDVI values. The maximum number of valid pixels was 62 612, corresponding to the image of February 1988; the difference between this number and the number of valid pixels of each image was calculated. These differences averaged 5%, with a standard deviation of 3.8% and a maximum of 19.1% corresponding to July 1984. This error was propagated to different operations like spatial distribution and multinomial analysis. In the evaluation of geographical changes, the total number of pixels was different for each pair of images, and only those pixels in classes A or B in both images were considered. This generated an error of 13.2–17.0% for changes from winter to spring, 5.6–8.6% for spring–summer changes, and 1.0–5.6% for summer–autumn changes.

These missing pixels did introduce an error in the median methodology proposed in this paper. The artefact pixels modified the frequency distribution. Consequently, the median of this distribution was modified as well. The maximum error in the context of this data set can be estimated from the influence of the difference between the maximum and minimum number of pixels (11 870). This difference introduced a bias in the estimated median. The frequency corresponding to the median could shift at most half of the difference mentioned (5935 pixels). This implied that the median would be 145 instead of 148 in July 1984. It should be noticed that this maximum estimated error (11 870 pixels) occurred only once in 108 images. The 70% of these errors had values under 4000 pixels, which resulted in a maximum error of 6.4% in image size.

The only artefacts included were those that had generally uniform and higher values than expected. Consequences of these artefacts appeared in the spatial analysis, which yielded unexpected NDVI values in southern Argentina from winter to spring of the 1987–1988 cycle (**Figure 6**), and also in the climatic significance analysis, which showed unexpected probabilities of pixels in class A belonging to semiarid and humid areas (**Figure 7a**). These artefacts were not present in the full set of 108 images, only in 14% of them.

Discussion

Histogram pattern analysis: dynamics and separation of the two modes

Histogram shape proved to be an effective means of illustrating the dynamic aspects of the growing cycle. This shape changed and accentuated higher values during spring and summer. Changes in the shape of peaks along the cycle, particularly for subset B, gave a kind of animation, a moving quick look at how images were changing in the NDVI values (**Figure 3**). Median values were in between the peaks of the histograms (valley), indicating that using the median as a split-up criterion was correct in the context of this data set.

The shifting of peaks A and B towards lower values in January and March 1988 was in agreement with decreasing mean NDVI values (**Figure 4a**) and with regional droughts in northern Argentina (Bobba, 1998; Bolsa de Cereales, 1989; González Loyarte and Menenti, 2000). The analysis of some meteorological stations (Instituto Nacional de Estadística y Censos, 1993) showed that there were monthly below-average rainfalls from December 1987 to April 1988, showing an irregular and different pattern each month. This fact might be reflected in the shifting of both peaks, with the shape of peak B changing as well.

Mean NDVI values showed cyclic changes. There was a difference in amplitude (difference between minimum and

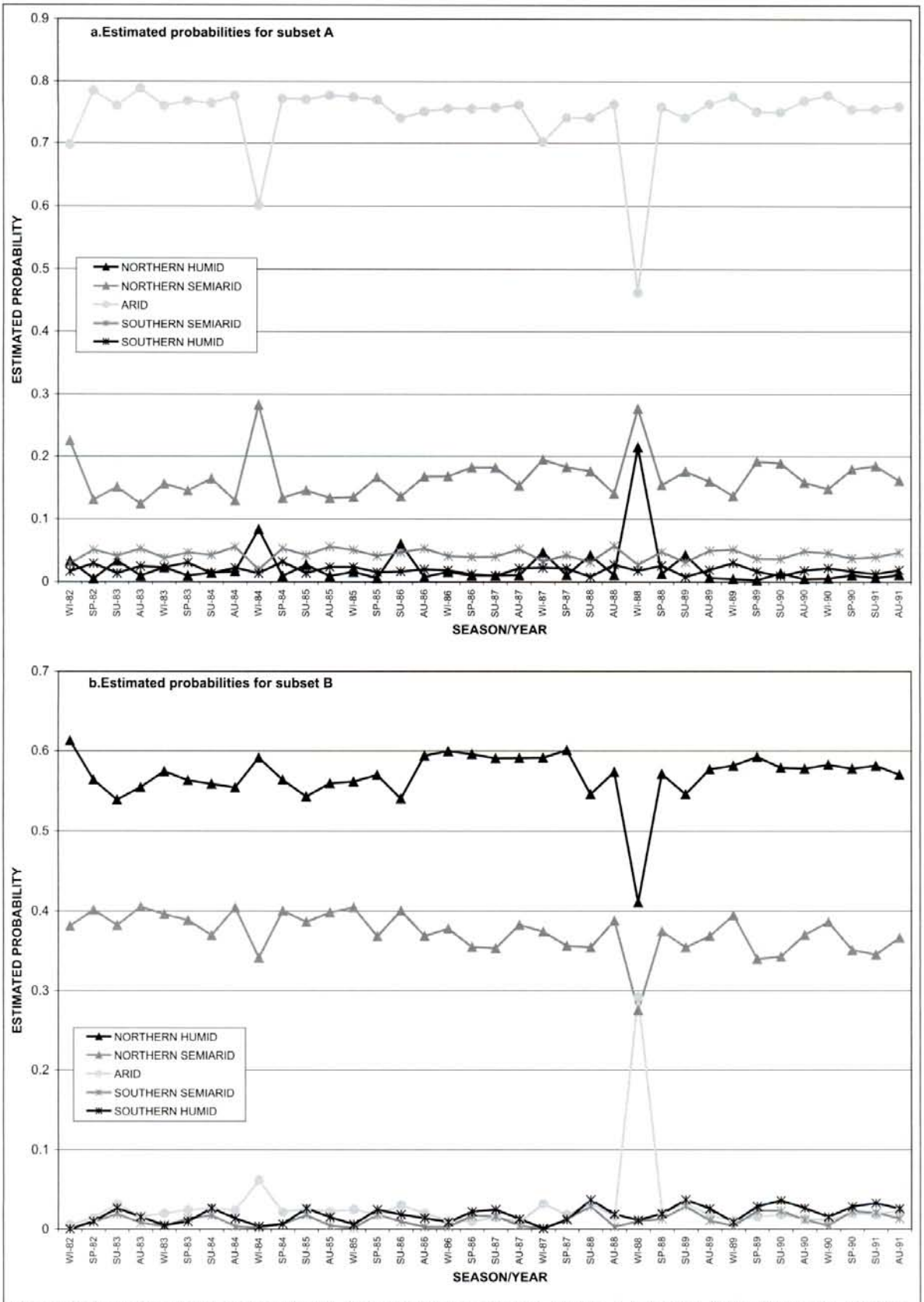

Figure 7. Seasonal evolution of estimated probabilities that pixels in subsets A (a) and B (b) belong to the different climatic zones. AU, autumn; SP, spring; SU, summer; WI, winter. A total probability of 1 was obtained for each season.

Table 2. Nine years average and standard deviation (SD) values of estimated probabilities that pixels in subsets A or B belong to each of the climatic zones.

		Climatic zones				
Subset	Statistics	Arid	Northern semiarid	Southern semiarid	Northern humid	Southern humid
A	Average	0.7464	0.1678	0.0429	0.0238	0.0190
	SD	0.0583	0.0356	0.0160	0.0371	0.0063
B	Average	0.0287	0.3721	0.0115	0.5692	0.0185
	SD	0.0463	0.0260	0.0083	0.0329	0.0104

maximum values) between the modes (**Figure 4a**). Subset B presented a higher mean NDVI amplitude than did subset A. The low variation of dryland vegetation was mainly due to the permanent and sclerophyllus cover of shrubby steppe (Cabido et al., 1993) and to the low vegetation cover throughout the year. Mean NDVI values showed regular cycles except during irregular rains. The mean NDVI value for each mode dropped in January and March 1988, coinciding with droughts in northern Argentina (Bobba, 1998; González Loyarte and Menenti, 2000).

The pattern of standard deviation (SD) for bimodal histograms showed cyclic changes similar to those of the mean NDVI values. The standard deviation of bimodal histograms increased with the growing cycle, reaching the highest dispersion in summer where the contrast between vegetation cover and biomass of arid and humid areas was maximal (**Figure 4b**). The lowest SD was reached in winter. When there was an irregular distribution of rainfall (December–January 1988 and 1989 and January 1990), the value of SD decreased, concomitantly with regional droughts (Bobba, 1998; Bolsa de Cereales, 1989; González Loyarte and Menenti, 2000).

The evolution of the SD of modes A and B showed an opposite pattern. For subset A the maximal dispersion is reached in summer and the minimal in winter, with a relatively constant variation between cycles. By contrast, subset B showed frequent fluctuations in SD resulting in irregular cycles. Despite these fluctuations, maximal dispersion of NDVI was reached in spring, mostly because of the large extent of mode B which covered both semiarid and humid areas, because spring is the beginning of the rainy season in northern Argentina and rains may not be homogeneous, and because the mountain deciduous forests start sprouting in spring. Consequently, phenological differences were rather large in this season. The minimal value of SD for subset B was sometimes reached in winter and sometimes in summer. During the extensive period of very irregular rains that resulted in serious regional droughts in northern Argentina in 1988–1989 (Bobba, 1998) (from September 1987 to April 1990), the value of SD fluctuated and was relatively low. This might indicate the extent, and in some way the continuity, of droughts.

Geographical distribution of the two modes of bimodal histograms and their dynamics across selected growth cycles

The median is the midpoint of a distribution, the point such that half of the observations fall above it and half below (Moore and McCabe, 1989). Therefore, 50% of the pixels of recoded NDVI images will belong to class A, and the other 50% to class B. This percentage was in fact a little higher for class A because it included those pixels with the median value.

From one season to the next some pixels shift from class A to class B and vice versa. Statistics for seasonal changes along the two selected cycles showed that most pixels of each class, over 42% of the total image for each subset, remained in the same class (**Table 1**). The other pixels, 8.79–14.4%, changed from one class to the other. For the cycle with droughts, 1987–1988, the average of changing pixels (12.93%) was higher than that of the normal cycle, 1982–1983 (8.98%). This fact might help detect areas subject to higher risk of droughts or desertification processes if there were particular areas where a B for A substitution was made frequently during spring–summer. This aspect needs to be analysed in future studies.

To understand why those pixels became temporarily part of the other class, it was necessary to analyse where and when the changes took place (**Figure 6**). The evaluation of A–B changes from one season to the next was done with the support of a previous land use map (González Loyarte, 1996). Some meaningful classes were selected from this map (**Figure 8**).

The 1982–1983 cycle

For the 1982–1983 cycle, changes were concentrated in the northern semiarid zone, although they appeared in all of the climatic zones. Data on seasonal evolution for each cereal crop were taken from Bolsa de Cereales (1983).

Changes from winter to spring

Changes from class A in winter to class B in spring were related to irrigated oases of central western Argentina, semiarid grasslands, and semiarid forests. Rains started in spring, increasing vegetation cover in the two semiarid environments. In the humid areas, some green patches appeared in the corresponding map (**Figure 6**) associated with mountain forests with deciduous trees in the south, and with intensive rain-fed agriculture in the north. In areas with intensive rain-fed agriculture, wheat was seeded in July–August, with good rains occurring in September–October 1982 (Bolsa de Cereales,

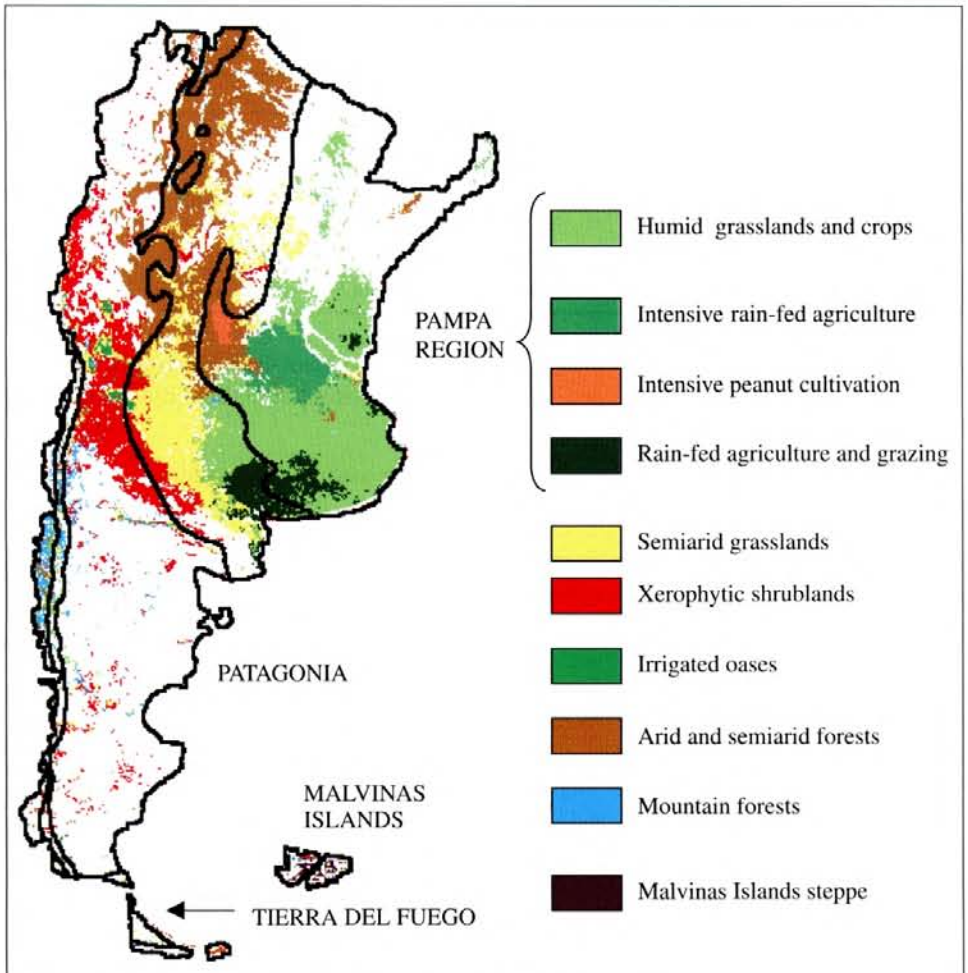

Figure 8. Land use map. Adapted from González Loyarte (1996).

1983), and therefore the new plant cover was reflected by the change from class A to class B. Also, climatic conditions for maize were good for areas corresponding to semiarid grasslands and intensive peanut cultivation.

Among the small red patches in the map, where pixels shifted from class B to class A, those coinciding with the intensive peanut cultivation area (95% of the national production; Bolsa de Cereales, 1983) were explained by soil ploughing from September to October 1982, as the land was being prepared for the next seeding. In this area, cultivation of peanuts is rotated with other crops like maize, sorghum, soya bean, sunflower, or perennial grasses (Pedelini, 1998). Therefore, there were areas where crops had been recently harvested and others with permanent grassland. This could explain the changes from class A in winter to class B in spring, or the maintenance of class B in both seasons. The harvest of maize, sorghum, or soya bean ends in May–June, and thereafter comes a fallow season where stubble is left in the soil until ploughing and kept resting for 2 months prior to seeding to increase yields. This could account for the initial pixels of class A (yellow) in the peanut nucleus corresponding to soils that were almost bare, ploughed, or covered with dry vegetation.

Changes from spring to summer

The arid forest increased its greenness (from class A to class B) in response to a good rainy season. Also, the peanut nucleus increased its plant cover because seeding started in November 1982 and finished by mid-December, and healthy plants developed as a result of the January rains. In the south, mountain forests increased their cover, and so also did the steppe and forests in Tierra del Fuego Island and the steppe in Malvinas Islands (Roig, 1998).

Among the areas that showed less healthy vegetation (from class B to class A) were those corresponding to semiarid grasslands. Here there was scarce rainfall since December, which affected the development of maize that bloomed in underdeveloped plants, suggesting a reduction in yield.

The decline in NDVI values, in agreement with the rain-fed agriculture and grazing class, can be explained by crop dynamics. Farms (covering over 200 ha) in this area combine permanent pastures for cattle grazing and rotating crops, primarily wheat, sunflower, maize, barley for beer, and sorghum (Cascardo et al., 1991). Possibly, a combination of December–January droughts and harvest effects occurred. In January 1983, plant cover diminished as the harvesting of wheat and barley was over. This effect may have been

reinforced by the ending of sunflower seeding in December 1982 with scarce rains and low maize growth under drought conditions. The broad pixel covered 5776 ha and therefore included many farms and combinations of land use.

In the intensive rain-fed agriculture area, 60–70% of the surface was cultivated with soya bean, 30% with maize, and 20–35% with rotating crops of wheat – soya bean (Cascardo et al., 1991). Because of good rains, the seeding of maize was finished during November 1982; however, rains were scarce in December 1982 and January 1983 and affected maize growth. Another factor that may have contributed to the shift from class B to class A was that the seeding of soya bean, the main crop of the area, started in November because of the good climatic conditions, but drought conditions in December and January prevented seeding as planned. In addition, by January 1983 the harvest of wheat was finished, further contributing to the decrease in plant cover.

Droughts could also be the explanation for red patches (**Figure 6**) corresponding to humid grasslands and crops. In contrast, the small red dots in northeastern Argentina represent swampy areas (Escobar and Capurro, 1988) flooded after intense rains (Bolsa de Cereales, 1983).

Changes from summer to autumn

From February to April rains increased and most red pixels came back to class B, showing the reaction of summer crops (maize, soya bean, sunflower, and sorghum) to rain. Semiarid grasslands also showed a good recovery.

For the peanut nucleus, climatic conditions were good in February and crops continued to develop. Plants were harvested during March and April. This was not reflected in the NDVI values, which remained in class B, probably because in adjacent lands rotating crops and perennial grasses were growing. In March–April 1983 maize was harvested. Farms in this type of intensive agricultural land are mostly small to medium in size (50–300 ha) (Cascardo et al., 1991). Therefore, each pixel is a synthesis of many farms masking expected NDVI values.

The red–yellow strip in the map corresponds to the Paraná River delta, the persistence of which in class A, and the new changes from B to A, should be analysed in depth, since it is a flood-prone area. Flooded areas in the northeast of the country persisted.

The 1987–1988 cycle

During the 1987–1988 cycle, important changes from one class to the other were registered, mainly in semiarid zones (**Figure 6**). Data on the monthly evolution for each cereal crop were taken from Bolsa de Cereales (1988).

Changes from winter to spring

Increased greenness (from class A to class B) was related to irrigated oases, semiarid grasslands, the Pampa region, and mountain forests. In the Pampa region and semiarid grasslands rains were irregular, with good rains in August but droughts in September. Rains increased at the end of October 1987, allowing the seeding of maize, sorghum, and soya bean and the end of barley seeding; wheat already presented good development.

The decline in NDVI was registered in the northern semiarid zone, where significant droughts occurred in September and October and affected arid and semiarid forests and crop development. In northwestern Argentina there was a great economic interest in soya beans, and an important soil tillage started in September under very dry conditions, promoting soil erosion by wind. Droughts also affected the early seeding of maize and sunflower.

In the peanut nucleus, also experiencing drought conditions, soils were tilled in September and October. The yellow central area in the map indicated those pixels which were in class A also in winter, probably coinciding with the already harvested crops like maize, sorghum, and soya bean. These crops were harvested from April to June 1987, producing bare soils in July (Bolsa de Cereales, 1987). The red areas can be explained by the significant droughts that may have affected the development of the rotational perennial grasses and also by the interest in cultivating soya beans (transforming grasslands into new crops). The cultivated surface of soya beans in this area increased 19.5% compared with that for the 1986–1987 cycle (Bolsa de Cereales, 1988).

Changes from spring to summer

Changes from class A to class B were coincident with the drought-affected areas in early spring. The improvement in vegetation cover was due to the occurrence of rainfall from November to January in the northwestern region. In the peanut nucleus, peanut seeding finished in December and blooming occurred in January 1988, with an excellent vegetation status.

Changes from class B to class A were localized in the northern humid and semiarid zones. In the area with intensive rain-fed agriculture and northwards, seeding of sorghum finished in December after the good November rains. During January there were no rains, which affected almost the entire sorghum area, in agreement with the red patches (**Figure 6**). Wheat harvest started by mid-November 1987 and ended by mid-January 1988, contributing to the reduction of plant cover.

The red area related to rain-fed agriculture and grazing and semiarid grasslands appeared more consolidated than in the 1982–1983 cycle. In the rain-fed agriculture and grazing area, the harvesting of wheat and barley for beer ended by mid-January 1988. Abundant rains from the end of October to December furthered excellent development of the maize crop. Despite the good rains, the presence of pixels in class A in this area suggested that harvest of wheat and barley had a strong influence on total vegetation cover. In the semiarid grassland area, climatic conditions were very different; after the rains at the end of October, there were no rains but only dry and hot winds during December and January and a late frost in January that affected crop development. It is worthwhile analysing some areas in depth and trying to distinguish between the effects of droughts and those of harvests.

Changes from summer to autumn

In most areas of the humid zone that had suffered the effects of droughts and harvesting, despite the irregular rains during this period, the conditions of the maize and sorghum crops improved, changing from class A to class B.

In the semiarid region, where red patches coincided with semiarid grasslands, January droughts extended to February, affecting the late seeding of sorghum. Consequently, sorghum fields were devoted to grazing. Therefore, red patches were new zones added to the previous ones (spring–summer), the latter remaining in class A (yellow class). As a result of the adverse climatic events since December, the maize yield was reduced by 29% compared with the 1986–1987 cycle (Bolsa de Cereales, 1988).

For southern Argentina, autumn seemed to start in the forests and the grassland steppe of Tierra del Fuego Island and Malvinas Islands, changing from class B to class A. In the arid zone, oases and cultivated valleys started to show the effects of autumn.

Thus, changes from class A to class B were considered to be a consequence of an improvement in water supply (rainfall or irrigation) combined with good temperatures for plant growth. Changes from class B to class A reflected a reduction of vegetation cover produced by droughts, harvests, or seasonal changes (autumn).

Climatic significance of bimodal histograms: multinomial statistical analysis of subsets A and B

A relationship was found between modes and climatic conditions. For subset A the highest probability, 74.6% on average for all nine cycles, was found for the arid zone, followed by the semiarid zones (21.1%) (**Table 2**; **Figure 7**). Humid areas had the lowest probabilities of being integrated by subset A (4.3%). The exception to this pattern is presented in the winter of the 1984–1985 and 1988–1989 cycles because of cloud artefacts.

Artefacts, generally with higher values than the median, strongly modified the probabilities because of the increase in the number of pixels in subset B. As a consequence, subset A lost pixels and reduced its probability of belonging to the arid zone, increasing that of belonging to semiarid and humid zones. These artefacts were located in the arid zone of Patagonia. Therefore, the probability of pixels in subset B belonging to the arid zone increased for the winters of 1984 and 1988 (**Figure 7b**). The artefacts for the winter of 1984 were also located in the Pampa region. As a result, the probability of pixels in subset B belonging to the northern humid zone also increased.

A contrast in behaviour was clear for subset B. Pixels of subset B had the maximum probability of belonging to humid zones (58.8%) and then to semiarid zones (38.4%). The arid zone had the lowest probability of having pixels of subset B (2.9%). Probabilities of belonging to humid zones increased at the expense of those belonging to semiarid and arid zones. The influence of artefacts was also clear.

It is worth mentioning that the lowest probabilities showed significant seasonal variations. For subset A, in autumn and winter, the probability of belonging to southern semiarid and humid zones increased (**Figure 7a**). This was explained by the fact that mountain deciduous forests lost leaves. During spring and summer, this probability decreased because pixels shifted to subset B as vegetation cover increased. The increased probabilities of pixels in subset A belonging to northern humid zones for some summers was due to a temporary decline in vegetation cover caused by drought in northern humid zones, as in the summer of 1986 in northeastern Argentina and the summer of 1989 in the Pampa region (Instituto Nacional de Estadística y Censos, 1993). For subset B, lower probabilities of belonging to southern semiarid and humid zones occurred in winter, and higher probabilities in summer. The reduction in winter was because pixels in subset B shifted to subset A as soon as the cold season reduced plant cover. Higher probabilities were due to the shift of pixels in subset A to subset B in summer in mountain deciduous forests, which increased the probability of belonging to south semiarid and humid zones. Also, in the arid zone there were pixels in subset A from oases that shifted to subset B in spring–summer and autumn, as discussed earlier in the paper.

Conclusions

The analysis of bimodal histograms yielded interesting results. The proposed methodology to split up bimodal histograms using the median, in the Argentinian context, was useful. The median, as a split-up criterion, over the nine growing cycles gave coherent results when these were checked with other sources of information. The two modes of the histograms showed the dynamics of vegetation cover across growth cycles. These dynamics were shown by the changing shape of monthly histograms and their statistical parameters. Both aspects were sensitive to special events like regional droughts. Artefacts with unusually high NDVI values were present in 14% of the images and affected the observed frequency distribution. Errors produced by missing data due to snow–cloud cover and ancillary data, such as political boundaries and coordinates, were at most 6.4% in image size, for 70% of the images.

The ecological meaning of modes was dynamic and complex. About 84% of pixels remained in the same mode, and 16% shifted temporarily from one mode to the other. Bimodal histograms, for the Argentinian context, were a phenological answer to climatic conditions but were not related to north–south rainfall areas. For mode A the highest probability was to belong to the arid zone (74.6%), then to semiarid zones (21.1%); the lowest probability was to belong to humid zones (4.3%). The exception to this pattern was presented in the winter of the 1984–1985 and 1988–1989 cycles because of artefacts with high NDVI values. Pixels of subset B, in contrast, had the maximum probability of belonging to humid zones (58.8%) and then to semiarid zones (38.4%); the lowest probability was to belong to the arid zone (2.9%). These

probabilities changed in the winter of the 1988–1989 cycle due to artefacts with high NDVI values.

The spatial analysis of the modes allowed us to understand the dynamics of vegetation cover. Periodic spatial changes of modes, and eventual spatial changes, showed areas where vegetation cover was more dynamic. Semiarid zones were more dynamic in terms of the phenological changes of modes and the variation in probabilities along the time series. Pixels that coincided with semiarid zones presented a constant shifting of modes across the growing cycle. Changes from mode A to mode B were considered to be a consequence of an improvement in water supply (rainfall or irrigation) combined with good temperatures for plant growth. Changes from mode B to mode A were considered to be a consequence of a reduction of vegetation cover produced by droughts, harvests, or seasonal changes (autumn).

Improving the knowledge of multimodal histograms may allow a better understanding of classification results. In this contribution a very simple classification criterion was presented: the splitting up of the two modes of the histograms. This helps to understand the dynamics of vegetation cover along the latitudinal range from 22° to 55°S for nine growing cycles.

Acknowledgements

To the memory of Julia Loyarte Yagüe, my mother, and my friend and colleague María Barton, who must certainly be encouraging this women's project from heaven. I am very grateful to several colleagues: to Dr. Massimo Menenti, who adhered to this project and forwarded me the invitation from European colleagues to join this venture; to Dr. Angela M. Diblasi for her valuable support in the statistical analysis; to Prof. Nelly Horak for her careful English corrections; to Eng. Claire Jacobs for her criticism and friendship; to Prof. María Elina González de Roccasalva for her accurate translation to French; to Prof. María Cecilia Scoones for histogram drawing; to Mr. Rubén Soria from CRICYT Informatics Service for making ASCII data compatible from ERDAS to STATISTICA, and to Mrs. Rosemary Torpeess who supported me throughout the project. Special thanks to Dr. Behnaz Zand-Rodríguez, whose knowledge and thorough explanations of satellite imagery imparted during my UNITAR training period in Geneva continue to be a constant support. Financial support was provided by the European Communities project "Impact of Climate Variability on Agro-ecosystems and Water Resources in Drylands" (CLIWARDA).

References

Azzali, S.M. 1990. High and low resolution satellite images to monitor agriculture land. Report 18, Winand Staring Centre, Wageningen, The Netherlands. 90 pp.

Azzali, S., and Menenti, M. 1996. Fourier analysis of time series of NOAA-AVHRR NDVI monthly composites for monitoring vegetation–soil–climate complexes in Southern Africa. In: Azzali, S., and Menenti, M. (Editors), *Fourier analysis of temporal NDVI in the Southern African and American continents*. Report 108, Winand Staring Centre for Integrated Land, Soil and Water Research, Wageningen, The Netherlands, pp. 37–81.

Azzali, S., and Menenti, M. 1999. Mapping isogrowth zones on continental scale using temporal Fourier analysis of AVHRR NDVI data. *International Journal of Applied Earth Observation and Geoinformation*, Vol. 1, No. 1, pp. 9–20.

Azzali, S., and Menenti, M. 2000. Mapping vegetation–soil–climate complexes in southern Africa using temporal Fourier analysis of NOAA-AVHRR NDVI data. *International Journal of Remote Sensing*, Vol. 21, No. 5, pp. 973–996.

Bobba, M.E. 1998. Detección de las sequías climáticas en el Noroeste Argentino. *GAEA (Sociedad Argentina de Estudios Geográficos), Contribuciones Científicas 1998*.

Bolsa de Cereales. 1983. Número Estadístico 1983. Bolsa de Cereales, Buenos Aires, Argentina, pp. 37–294.

Bolsa de Cereales. 1987. Número Estadístico 1987. Bolsa de Cereales, Buenos Aires, Argentina, pp. 98–241.

Bolsa de Cereales. 1988. Número Estadístico 1988. Bolsa de Cereales, Buenos Aires, Argentina, pp. 52–278.

Bolsa de Cereales. 1989. Número Estadístico 1989. Bolsa de Cereales, Buenos Aires, Argentina, pp. 60–223.

Bruniard, E.D. 1982. La diagonal árida argentina: un límite climático real. *Revista Geográfica IPGH*, No. 95, pp. 5–20.

Cabido, M., González, C., Acosta, A., and Díaz, S. 1993. Vegetation changes along a precipitation gradient in central Argentina. *Vegetatio*, Vol. 109, pp. 5–14.

Cascardo, A.R., Pizarro, J.B., Peretti, M.A., and Gómez, P.O. 1991. Sistemas de producción predominantes. In: Barsky, O. (Editor), *El desarrollo agropecuario pampeano*. Grupo Editor Latinoamericano, Buenos Aires, pp. 95–146.

De Martonne, E. 1948. *Traité de géographie physique*. Librairie Armand Colin, Paris, Vol. 1, Chapt. 7, pp. 287–301.

Diallo, O., Diouf, A., Hanan, N.P., Ndiaye, A., and Prévost, Y. 1991. AVHRR monitoring of savanna primary production in Senegal, West Africa: 1987–1988. In: Price, S.D., and Justice, C.O. (Editors), Coarse resolution remote sensing of the Sahelian environment. *International Journal of Remote Sensing (Special Issue)*, Vol. 12, No. 6, pp. 1259–1279.

Diblasi, A.M. 1999. Multinom. MATLAB Programme CRICYT, Mendoza, Argentina.

Escobar, E.M., and Capurro, R.A. 1988. Provincia de Corrientes. In: PROSA (Editor), *El Deterioro del Ambiente en la Argentina*. FECIC Editorial, Buenos Aires, pp. 79–83.

Franklin, J., and Hiernaux, P.H.Y. 1991. Estimating foliage and woody biomass in Sahelian and Sudanian woodlands using a remote sensing model. In: Price, S.D., and Justice, C.O. (Editors), Coarse resolution remote sensing of the Sahelian environment. *International Journal of Remote Sensing (Special Issue)*, Vol. 12, No. 6, pp. 1387–1404.

González Loyarte, M.M. 1995. La diagonale aride argentine: une realité écologique oscillante. *Sécheresse*, Vol. 6, No. 1, pp. 35–44.

González Loyarte, M.M. 1996. Study of the variability of vegetation cover in Argentina. In: Azzali, S., and Menenti, M. (Editors), *Fourier analysis of temporal NDVI in the Southern African and American continents*. Report

108, Winand Staring Centre for Integrated Land, Soil and Water Research, Wageningen, The Netherlands, pp. 83–112.

González Loyarte, M.M., and Menenti, M. 2000. Usefulness of Fourier parameters to detect regional and local droughts within a time series of NOAA/AVHRR-NDVI data (GAC). In: Roerink, G.J., and Menenti, M. (Editors), *Time series of satellite data: development of new products*. NRSP-2 Report 99-33, ALTERRA Green World Research, Wageningen, The Netherlands, pp. 63–70.

Hoffmann, J.A.J. 1975. *Atlas climático de América del Sur, WMO-UNESCO*. Cartographia, Budapest, Hungary, 9 pp., 28 maps.

Instituto Nacional de Estadística y Censos (INDEC). 1993. *Anuario Estadístico de la República Argentina 1993*. Instituto Nacional de Estadística y Censos, Buenos Aires, Argentina, pp. 11–16.

Jensen, J.R. 1989. *Introductory digital image processing. A remote sensing perspective*. Prentice-Hall Inc., Englewood Cliffs, N.J. 379pp.

Justice, C.O., Townshend, J.R.G., Holben, B.N., and Tucker, C.J. 1985. Analysis of the phenology of global vegetation using meteorological satellite data. *International Journal of Remote Sensing*, Vol. 6, No. 8, pp. 1271–1318.

Justice, C.O., Dugdale, G., Townshend, J.R.G., Narracott, A.S., and Kumar, M. 1991. Synergism between NOAA-AVHRR and Meteosat data for studying vegetation development in semi-arid West Africa. In: Price, S.D., and Justice, C.O. (Editors), Coarse resolution remote sensing of the Sahelian environment. *International Journal of Remote Sensing (Special Issue)*, Vol. 12, No. 6, pp. 1349–1368.

Menenti, M., Azzali, S., Verhoef, W., and van Swol, R. 1991. Mapping agroecological zones and time lag in vegetation growth by means of Fourier analysis of time series of NVI images. Report 32, DLO Winand Staring Centre, Wageningen, The Netherlands. 42 pp.

Miller, R.G. 1981. *Simultaneous statistical inference*. 2nd ed. Springer-Verlag, New York.

Moore, D.S., and McCabe, G.P. 1989. *Introduction to the practice of statistics*. W.H. Freeman and Company, New York. 790 pp.

Pedelini, R. 1998. Suelo, Siembra, Crecimiento y Desarrollo del cultivo del maní. In: Pedelini, R., and Casini, C. (Editors), *Manual del maní*, 3rd ed. INTA-EEA Manfredi, Córdoba, Argentina, pp. 3–14.

Roig, F.A. 1998. La vegetación de la Patagonia. In: Correa, M.N. (Editor), *Flora Patagónica*. INTA Colección Científica, Tomo VIII, Vol. I, pp. 47–166.

Roig, F.A., Abraham de Vázquez, E.M. González Loyarte, M.M., Martínez Carretero, E., Méndez, E., Dalmasso, A.D., and Roig, V.G. 1988. Documento de base para un Plan Nacional de Acción para Combatir la Desertificación en la República Argentina. United Nations Environment Programme (UNEP), Desertification Control (PAC), Mendoza, Argentina. 89 pp.

Roig, F.A., González Loyarte, M.M., Abraham de Vázquez, E.M., Martínez Carretero, E., Méndez, E., and Roig, V.G. 1992. Maps of desertification hazards of central-western Argentina (Mendoza Province: study case). In: United Nations Environment Programme (UNEP) (Editor), *World atlas of desertification*. Edward Arnold, London, pp. 50–53.

Tucker, C.J., Newcomb, W.W., Los, S.O., and Prince, S.D. 1991. Mean and inter-year variation of growing-season normalized difference vegetation index for the Sahel 1981–1989. In: Price, S.D., and Justice, C.O. (Editors), Coarse resolution remote sensing of the Sahelian environment. *International Journal of Remote Sensing (Special Issue)*, Vol. 12, No. 6, pp. 1133–1135.

Wylie, B.K., Harrington, J.A., Jr., Prince, S.D., and Denda, I. 1991. Satellite and ground-based pasture production assessment in Niger: 1986–1988. In: Price, S.D., and Justice, C.O. (Editors), Coarse resolution remote sensing of the Sahelian environment. *International Journal of Remote Sensing (Special Issue)*, Vol. 12, No. 6, pp. 1281–1300.